Novel Multifunctional of Magnesium Ions (Mg^{++}) Incorporated Calcium Phosphate Nanostructures

K. Thanigai Arul [a*,1], M. Ramesh [b,*], C. Chennakesavan [c], V. Karthikeyan [c], E. Manikandan [d,e*], A. Umar [f], M. Maaza [e], M. Henini [g]

[a] Dept. of Physics, AMET University, Kanathur, Chennai-603112, Tamil Nadu (TN), India
[b] Functional Materials Division, CSIR-Central Electrochemical Research Institute, Karaikudi -630003, TN, India
[c] Dept. of Electrical and Electronics Engineering (Marine), AMET University, Kanathur, Chennai-603112, TN, India
[d] Dept. of Physics, TVUCAS Campus, Thennangur, 604408, Thiruvalluvar University, Vellore, TN, India
[e] UNESCO-UNISA Africa Chair in Nanosciences-Nanotechnology, College of Graduate Studies, University of South Africa, Muckleneuk Ridge, PO Box 392, Pretoria, South Africa
[f] Dept. of Chemistry, College of Science & Arts Promising Centre for Sensors and Electronic Devices, Najran University, PO Box1988, Najran-11001, Kingdom of Saudi Arabia
[g] School of Physics and Astronomy, Nottingham Nanotechnology and Nanoscience Center, University of Nottingham, Nottingham, NG7 2RD, United Kingdom

ABSTRACT

Magnesium ions incorporated calcium phosphate was synthesized by wet chemical route and followed by microwave assisted method. XRD analysis was confirmed that the presence of calcium phosphate (hydroxyapatite). TEM analysis was exhibited rod-like morphology. XRF results were showed the percentage of calcium, phosphate, magnesium and oxygen. There was a slight blue shift observed in magnesium ions based samples. Higher magnesium (0.1Mg-HAp) was revealed the greater discharging time with capacitance voltage (0.55 V). Magnesium based calcium phosphate was showed prolonged rate of drug release. At higher frequency, the Nyquist plot was showed the electrochemical behavior, however at lower frequency, revealed mass transfer process. Magnesium ions tailor the specific capacitance of calcium phosphate. Therefore, magnesium ions based phosphate samples could be an outstanding multifunctional candidate for drug release and supercapacitor applications.

[1*]Corresponding Authors:thanigaiarul.k@gmail.com (Prof.K. Thanigai Arul) rameshpondi108@gmail.com (Dr. M. Ramesh); maniphysics@gmail.com (Prof. E. Manikandan)

Keywords: Biomaterials; Hydroxyapatite; Metal-ions; Drug release; Electroschemical studies. Supercapacitor.

1. Introduction

Calcium phosphate ($Ca_{10}(PO_4)_6(OH)_2$, HAp) based bioceramics most often employed for bone and dental applications. HAp has been extensively employed for bone and dental replacement and also in drug delivery system. It reveals high osteoconductivity and osteoinduction when implanted in the human body [1]. Hydroxyapatite (HAp) is a dielectric material along with piezoelectric behaviour. Moreover, it can also be used for gas sensing, chromatographic agent etc. HAp solubility was varied by addition of different metal ions incorporation (Na^+, Mg^{2+}, Ba^{2+}, Sr^{2+} etc.). Among the metal ions, magnesium ions play an important role for formation of HAp [2]. Metal ion (magnesium) incorporation in calcium phosphate used for UV light emitting applications [3]. Nowadays, for enhancing energy and power demands, supercapacitor is playing crucial role. Supercapacitor is a latest generation of electronic tool to develop battery and capacitor performance in terms of power and energy density respectively. Supercapacitors are also known as electrochemical capacitors due to their superior rapid charge/discharge, long-term cycling stability [4].

Metal oxide (Mn_3O_4, RuO_2, NiO etc) based materials possess higher specific capacitance with lower stability [5,6]. Transition metal phosphates contain ammonium transition metal phosphates have been examined and used in many fields [7, 23-33]. Microwave assisted one-pot oil-in-water emulsion technique for the synthesis of mesoporous $Ni_xCo_{3-x}(PO_4)_2$ hollow shell for supercapacitor applications [8]. Supercapacitor stored and discharge electrical energy could be

due to electrical double layers development [9]. Carbon based materials such as CNTs have revealed anisotropic microstructure, porous networks, high electric conductivity etc. which were constructed as key candidates for supercapacitor electrodes [10-14]. For large-scale single-walled carbon nanotubes (SWCNTs) film with high electric conductivity were employed as supercapacitor electrodes [15]. In the current work, first time magnesium-calcium phosphate material used for supercapacitor and drug delivery applications.

2. Materials and methods

Magnesium ion incorporated calcium phosphate was synthesized by microwave assisted route. For the preparation of HAp, calcium nitrate tetrahydrate (1.0 M) was mixed in deionized water and then added to diammonium hydrogen phosphate (0.6 M) solution at constant (pH 10). Final solution subjected to microwave irradiation (900 W and 2.45 GHz) for 30 minutes and dried in hot air oven at 80 ° C. It was denoted as HAp. Different molar concentration of magnesium (0.01 and 0.1) was added separately to calcium nitrate tetrahydrate (1.0 M), drop wise added to diammonium hydrogen phosphate (0.6 M) (pH 10) and followed by microwave irradiation (similar procedure) for the synthesis of magnesium ion incorporated HAp. For 0.01 and 0.1 molar concentration of magnesium ion incorporated HAp was ascribed as 0.01Mg-HAp and 0.1Mg-HAp respectively.

The synthesized samples were analyzed by Bruker XRD CuK_{α} radiation (0.154 nm) with step size 0.02° in a continuous scan mode. The morphology and particle size of samples were investigated using a Schottky field emission source (FE-HRTEM, Carl Zeiss Libra 200HR). Elemental concentration of samples was measured using X-ray analytical microscope (HORIBA Scientific XGT-5200). For the drug release, the maximum absorbance wavelength (λ_{max}) of

amoxicillin as 230 determined using UV−Vis spectrophotometer. The *in vitro* release profile of amoxicillin was performed in phosphate buffer saline (PBS, pH 7.4) using incubated shaker. 100 mg of HAp, 0.01 Mg-HAp and 0.1Mg-HAp powder samples were mixed separately with amoxicillin (50 mg) and then pellets was made. The pellets were separately immersed into 200 mL of PBS solutions and maintained at 37 °C. At various time intervals, 1 mL of PBS was taken out and replaced with fresh medium. The concentration of the amoxicillin (released) was estimated from the calibration graph. The experiments were performed in triplicate.

The electrochemical properties of HAp, 0.01Mg-HAp and 0.1Mg-Hap were studied using with three electrode configurations. The electrode past was prepared in ratio 70:23:7, 70 of active material and 23 % of super p carbon and 7% of PTFE. The working electrodes was fabricated on nickel mesh by pressing the 5 mg past and dipped in 20 % KOH solution over night. The reference and counter electrode are Hg/HgO and Pt foil. Cyclic voltammetry and galvanostatic charge-discharge measurement were monitored in Biologic (VSP 300) instrument in 20% KOH electrolyte.

3. Results and Discussions

3.1. XRD analysis

XRD patterns of magnesium ion doped hydroxyapatite were as shown in Fig.1. The planes (002), (102), (210), (211), (202), (301), (221), (222), (312) and (213) were good agreement with jcpds value (09-0432) of HAp. On higher magnesium ion incorporation, the prominent plane (211) broadened due to lattice stress of HAp. Moreover, the plane (202) was diminished at higher incorporation of magnesium ion compared to other samples [16]. The average crystallite size was

calculated using MAUD (Material Analysis Using Diffraction). The crystallite size of HAp, 0.01 Mg-HAp and 0.1 Mg-HAp was 30±2 nm, 20±0.5 nm and 14±0.5 nm respectively. The decrease in crystallite size on magnesium ion incorporation could be due to the presence of magnesium ion in interstitial sites of HAp [16].

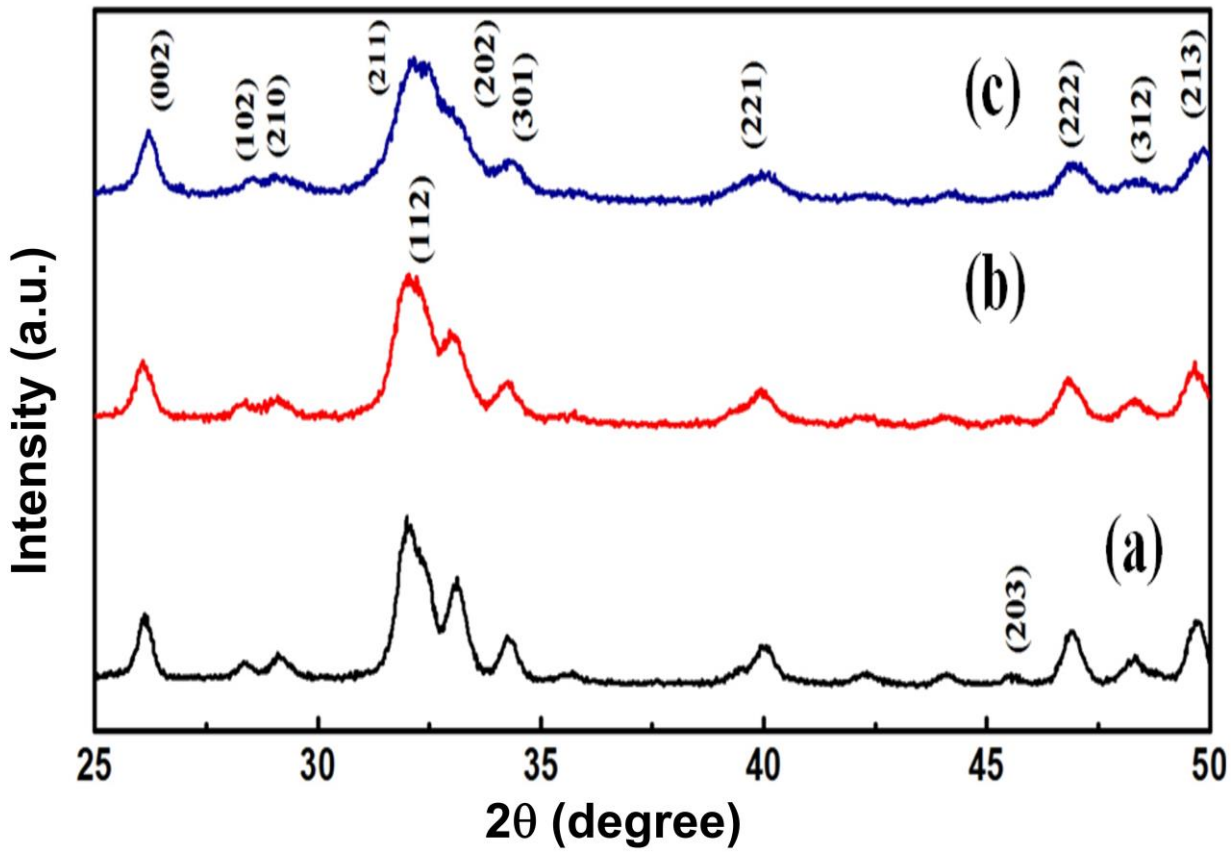

Fig.1 XRD patterns of (a) HAp, (b) 0.01Mg-HAp and (c) 0.1Mg-HAp

3.2. Transmission Electron Microscopy (TEM)

HR-TEM analysis was as shown in Fig.2. Pristine showed rod like morphology and its average particle size (approximately 29×7±3 nm). The particle size of 0.1 Mg-HAp was 23×5±4 nm. The decrease in particles size could be due to magnesium ion in interstitial sites of HAp that could modify the growth kinetics of HAp. M.H. Chen et al. reported that the particle size of

nanocrystal about 100 nm (length) and 30–40 nm (width) [17]. In our case, the length decreased by 77 % and width decreased by 87.5 % when compared with M. H. Chen et al.

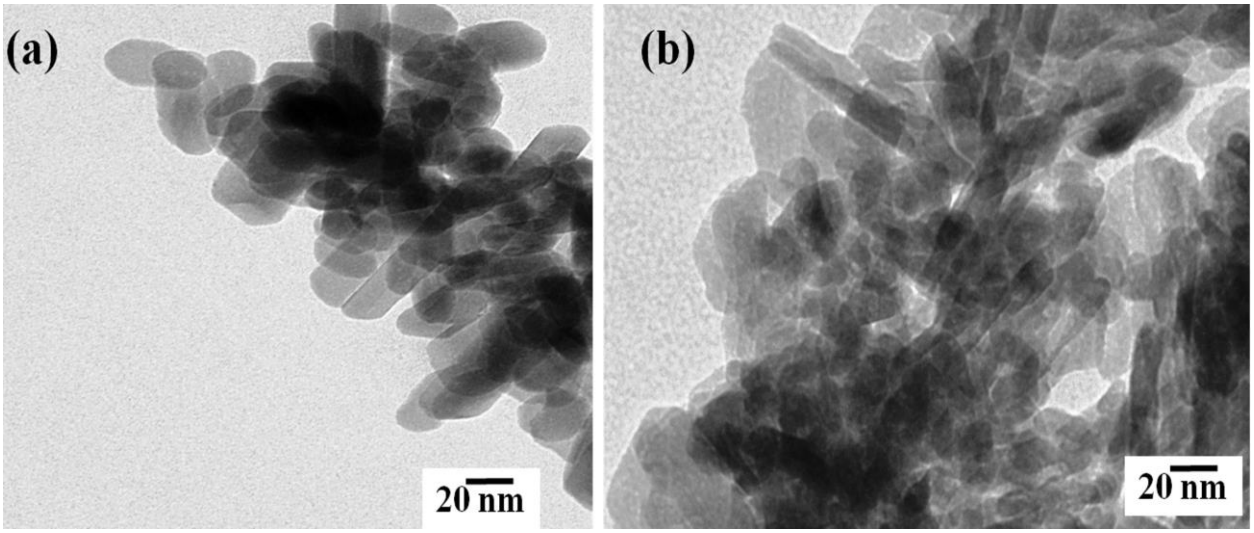

Fig. 2. HR-TEM analysis of pristine shows (a) rod-like morphology, (b) magnesium ion (Mg^{++}) in interstitial sites of HAp

3.3. XRF

XRF (X-ray Fluorescence) analysis of HAp and incorporated HAp was shown in Fig.3A. It was confirmed that the presence of calcium, phosphate and magnesium. Fig.3A (b, c) showed that the occurrence of magnesium ion incorporated samples. The percentage of calcium, phosphate, and oxygen in pristine was 36.11, 21.27 and 42.62 respectively. For 0.01Mg-HAp contains calcium (37.6 %), phosphate (20.39 %), oxygen (41.59 %) and magnesium (0.42 %). The sample (0.1Mg-HAp) having calcium (34.08 %), phosphate (20.93 %), oxygen (42.34 %) and magnesium (2.65 %).

3.4. UV-Vis spectroscopy analysis

UV absorbance of the samples was as shown in the Fig.3B. On magnesium ion incorporation, there was no significant variation observed in the absorbance percentage. However, the doped samples slightly shift towards blue side. Electrochemical impedance spectra (EIS) of samples were measured within the range of frequency from 100 kHz to 500 mHz as shown in the Fig. 3C. In Nyquist plot showed semicircle at high frequency which was followed by a straight line at low frequency which indicates electrochemical and mass transfer process respectively [16].

3.5. Drug studies

The drug release percentage of amoxicillin incorporated HAp and Mg-HAp samples was as shown in Fig.3D. The 0.1 Mg-HAp revealed rapid drug release at 10 h. Prolonged drug release observed in 0.01 Mg-HAp at 47 h could be due to more binding of Mg^{2+} ions with amoxicillin. As the magnesium ion incorporation increases, the percentage of drug release was enhanced due to lesser binding of drugs which tend to leach more magnesium ions [18]. The Mg-HAp has the potential candidate to deliver drugs efficiently at the pretentious tissues [19]. Normally, sustained release of drug has a trend to transport drug molecules to the targeted cells in a controlled manner [20]. The Mg^{2+} incorporated sample (0.01 Mg-HAp) were revealed prolonged rate of drug release in comparison with pristine and 0.1 Mg-HAp.

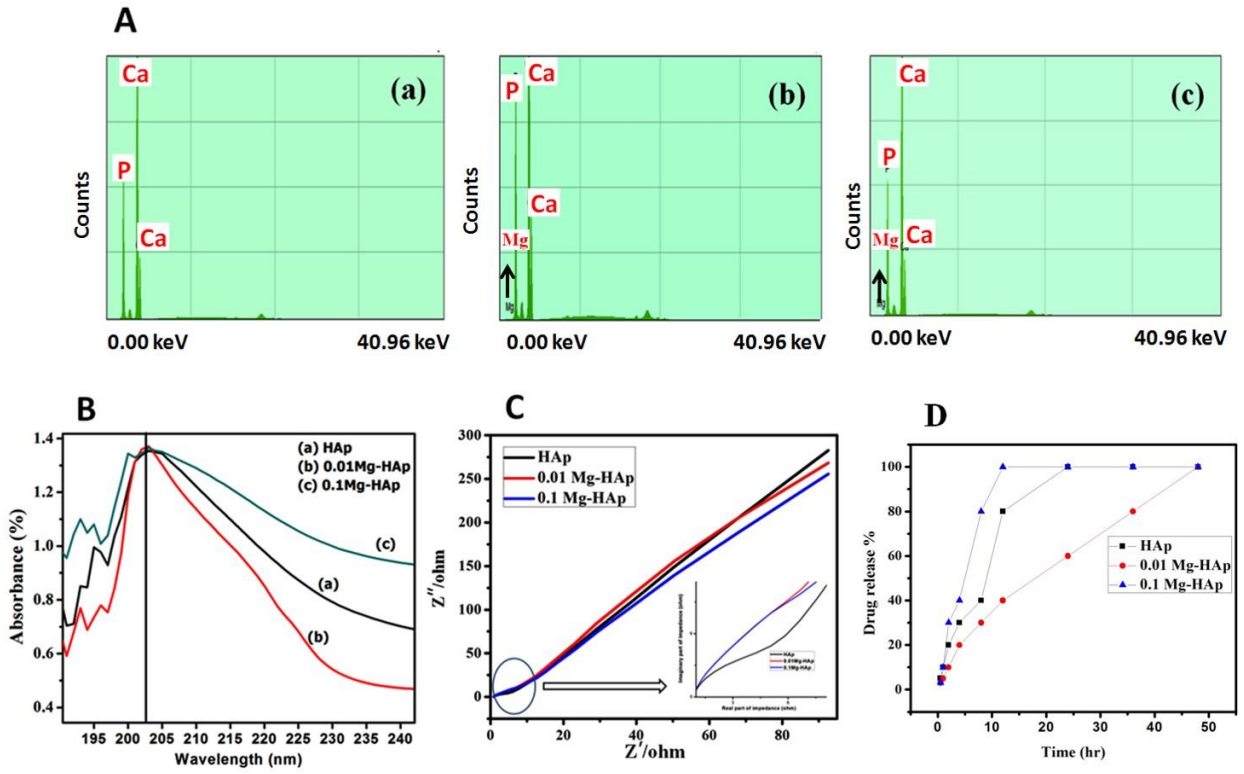

Fig.3 A. XRF analysis of (a) HAp, (b) 0.01Mg-HAp and (c) 0.1Mg-HAp, B. UV absorbance studies of (a) HAp, (b) 0.01Mg-HAp and (c) 0.1Mg-HAp. C. Real part of impedance versus imaginary part of impedance of samples. D. Drug release % for the pristine and Mg–HAp samples.

3.6. Electrochemical measurement

Electrochemical performance of the pure and ion incorporated samples was performed in 20 % KOH within a potential 0.05 to 0.6 V. Fig. 4 demonstrates the CV curves of the samples from 10 mV to 50 mV. There was strong peaks around 0.45 to 0.55 V and 0.35 to 0.45 V attained for all the samples and revealed the reversible Faradaic redox processes of magnesium in KOH solution

[22]. Fast current response to the voltage modulation is due to rapid electron transport. Fig. 5 showed the discharge curve of the samples at different current values which were exactly matches with CV results. The GCD (Galvanostatic Charge Discharge) curves of the samples were showed nearly symmetrical shape for various currents in a voltage window from 0 to 0.55 V which demonstrated superior electrochemical supercapacitor behavior. The specific capacitance of HAp, 0.01Mg-HAp and 0.1Mg-HAp was 28.6 F/g, 19.87 F/g and 11.56 F/g respectively which was calculated from charge-discharge curve. Linear profile of the charge-discharge curves of each samples was revealed ideal capacitive performance [22]. Magnesium ion incorporation in HAp enhances the discharging time and could be employed for supercapacitor application and still unclear to understand the mechanism.

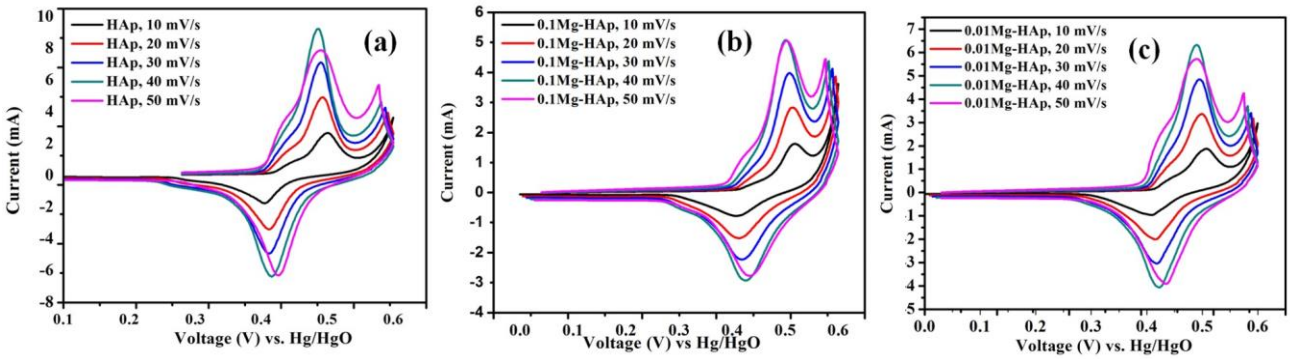

Fig.4 The cyclic voltammetry (CV) at different scan rate of (a) HAp, (b) 0.01Mg-HAp and (c) 0.1 Mg-HAp

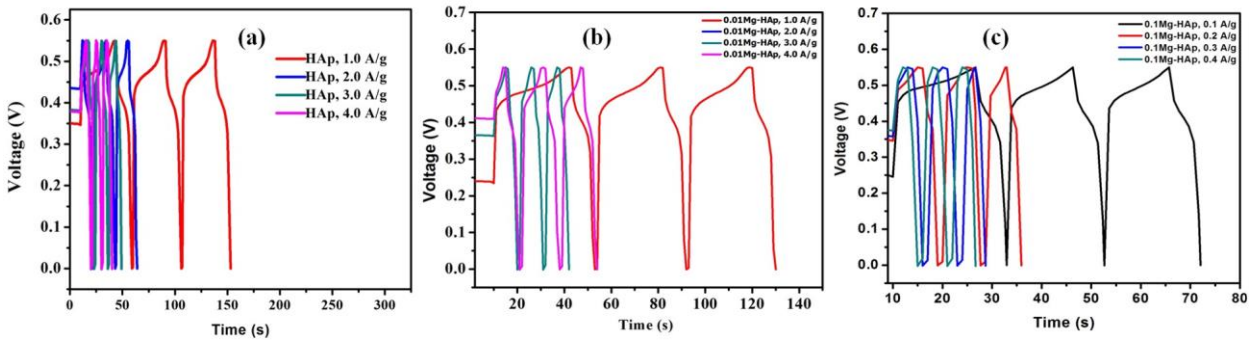

Fig.5 Galvanostatic charge/discharge curves of (a) HAp, (b) 0.01Mg-HAp and (c) 0.1 Mg-HAp under various electrochemical induced current.

4. Conclusions

Magnesium ions incorporated calcium phosphate was prepared by microwave assisted route. XRD analysis was confirmed that the presence of calcium phosphate (hydroxyapatite) with no phase change. Reduced rod like morphology observed on Mg-HAp samples. XRF confirmed that the percentage of calcium, phosphate, magnesium and oxygen. Optical studies were revealed that there was a slight shift towards blue side of the spectrum. Nyquist plot was revealed that the electrochemical behavior at higher frequency. Mg-HAp samples could aid in bone growth, healing of bone cracks and drug releasing properties. Strong peaks around 0.45 to 0.55 V and 0.35 to 0.45 V revealed the reversible Faradaic redox processes of magnesium. Charge-discharge curves of each sample were showed ideal capacitive performance. On magnesium ion incorporation which is able to tailor discharging time with specific capacitance 11.56 F/g along with multifunctional properties which could be useful as novel an electrode candidate for supercapacitor and biomedical applications.

Acknowledgements

Authors would like to thank the Department of Physics, AMET University, Chennai, Tamil Nadu, and thank Functional Materials Division, CSIR-Central Electrochemical Research Institute, Karaikudi, Tamil Nadu.

References

[1] J.A. Juhasz, S.M. Best, Bioactive ceramics: processing, structures and properties, J. Mater. Sci. 47 (2012) 610-624.
[2] K.T. Arul, J.R. Ramya, S.C. Vanithakumari, P. Magudapathy, U.K. Mudali, K.G.M. Nair, S. Narayana Kalkura, Novel ultraviolet emitting low energy nitrogen ion implanted magnesium ion incorporated nanocrystalline calcium phosphate, Materials Letters 153 (2015) 182-185.
[3] I.V. Fadeev, L.I. Shvorneva, S.M. Barinov, V.P. Orlovskii, Synthesis and Structure of Magnesium-Substituted Hydroxyapatite, Inorganic Materials 39(9) (2003) 947-950.
[4] J.R. Miller, P. Simon, Electrochemical Capacitors for Energy Management, Science 321(5889) (2008) 651-652.
[5] D. Dubal, D. Dhawale, R. Salunkhe, S. Pawar, V. Fulari, C. Lokhande, A novel chemical synthesis of interlocked cubes of hausmannite Mn_3O_4 thin films for supercapacitor application, Journal of Alloys and Compounds 484(1) (2009) 218-221.
[6] U. Patil, S. Kulkarni, V. Jamadade, C. Lokhande, Chemically synthesized hydrous RuO 2 thin films for supercapacitor application, Journal of Alloys & Compounds 509(5) (2011) 1677-1682.
[7] S.G. Carling, P. Day, D. Vissen, Crystal and Magnetic Structures of Layer Transition Metal Phosphate Hydrates, Inorganic Chemistry 34(15) (1995) 3917-3927.
[8] J. Zhang, Y. Yang, Z. Zhang, X. Xu, X. Wang, Rapid synthesis of mesoporous $Ni_xCo_{3-x}(PO_4)_2$ hollow shells showing enhanced electrocatalytic and supercapacitor performance, Journal of Materials Chemistry A 2 (2014) 20182-20188.
[9] X. Yang, C. Cheng, Y. Wang, L. Qiu, D. Li, Liquid-Mediated Dense Integration of Graphene Materials for Compact Capacitive Energy Storage, Science 341 (2013) 534-537.
[10] Y. Zhai, Y. Dou, D. Zhao, P.F. Fulvio, R.T. Mayes, S. Dai, Carbon materials for chemical capacitive energy storage, Advanced materials 23 (2011) 4828-4850.
[11] M. Kaempgen, C.K. Chan, J. Ma, Y. Cui, G. Gruner, Printable Thin Film Supercapacitors Using Single-Walled Carbon Nanotubes, Nano Letters 9 (2009) 1872-1876.
[12] S. Nardecchia, D. Carriazo, M.L. Ferrer, M.C. Gutierrez, F. del Monte, Three dimensional macroporous architectures and aerogels built of carbon nanotubes and/or graphene: synthesis and applications, Chemical Society Reviews 42 (2013) 794-830.
[13] S. Pan, J. Ren, X. Fang, H. Peng, Integration: An Effective Strategy to Develop Multifunctional Energy Storage Devices, Advanced Energy Materials 6(4) (2016) 1501867.
[14] B. Wang, X. Fang, H. Sun, S. He, J. Ren, Y. Zhang, H. Peng, Fabricating Continuous Supercapacitor Fibers with High Performances by Integrating All Building Materials and Steps into One Process, Advanced Materials 27(47) (2015) 7854-7860.

[15] Z. Niu, W. Zhou, J. Chen, G. Feng, H. Li, W. Ma, J. Li, H. Dong, Y. Ren, D. Zhao, S. Xie, Compact-designed supercapacitors using free-standing single-walled carbon nanotube films, Energy & Environmental Science 4(4) (2011) 1440-1446.
[16] I. Cacciotti, A. Bianco, M. Lombardi and L. Montanaro, Mg-Substituted Hydroxyapatite Nanopowders: Synthesis, Thermal Stability and Sintering Behavior, J. Eur. Ceram. Soc. 29 (2009) 2969-2978
[17] M.H. Chen, N. Hanagata, T. Ikoma, J.Y. Huang, K.Y. Li, C.P. Lin, F.H. Lin, Hafnium-doped hydroxyapatite nanoparticles with ionizing radiation for lung cancer treatment, Acta Biomaterialia, 37 (2016) 165–173
[18] V. Sarath Chandra, Kolanthai Elayaraja, K. Thanigai Arul, Sara Ferraris, Silvia Spriano, Monica Ferraris, K. Asokan, S. Narayana Kalkura, Synthesis of magnetic hydroxyapatite by hydrothermal–microwave technique: Dielectric, protein adsorption, blood compatibility and drug release studies, Ceramics International 41 (2015) 13153–13163
[19] J.Yang, C.H. Lee, H.J. Ko, J.S. Suh, H.G. Yoon, K. Lee, Y.M. Huh, S. Haam, Multifunctional magneto-polymeric nanohybrids for targeted detection and synergistic therapeutic effects on breast cancer, Angew. Chem. Int. Ed., 46 (2007) 8836-8839
[20] P. Yang, Z.Quan, C. Li, X. Kang, H. Lian, J. Lin, Bioactive, luminescent and mesoporous europium-doped hydroxyapatite as a drug carrier, Biomaterials 29 (2008) 4341-4347
[21] G.Q. Zhang, Y.-Q. Zhao, F. Tao, H.-L. Li, Electrochemical characteristics and impedance spectroscopy studies of nano-cobalt silicate hydroxide for supercapacitor, Journal of Power Sources 161(1) (2006) 723-729.
[22] Z. Wang, L. Pan, H. Hu, S. Zhao, Co_9S_8 nanotubes synthesized on the basis of nanoscale Kirkendall effect and their magnetic and electrochemical properties, CrystEngComm 12(6) (2010) 1899-1904.
[23] J Kennedy, A Markwitz, Z Li, W Gao, C Kendrick, SM Durbin, R Reeves. Modification of electrical conductivity in RF magnetron sputtered ZnO films by low-energy hydrogen ion implantation. Current Applied Physics 6 (2006) 495-498.
[24]. B Sathyaseelan, E Manikandan, K Sivakumar, J Kennedy, M Maaza. Enhanced visible photoluminescent and structural properties of ZnO/KIT-6 nanoporous materials for white light emitting diode (w-LED) application. Journal of Alloys and Compounds 651 (2015) 479-482.
[25] SAA Azis, J Kennedy, P Cao. Effect of annealing on microstructure of hydroxyapatite coatings and their behaviors in simulated body fluid. Advanced Materials Research 922 (2014) 657-662.
[26] E Manikandan, J Kennedy, G Kavitha, K Kaviyarasu, M Maaza. Hybrid nanostructured thin-films by PLD for enhanced field emission performance for radiation micro-nano dosimetry applications. Journal of Alloys and Compounds 647 (2015) 141-145.
[27] K Elayaraja, P Rajesh, MIA Joshy, VS Chandra, RV Suganthi, J Kennedy. Enhancement of wettability and antibiotic loading/release of hydroxyapatite thin film modified by 100MeV Ag 7+ ion irradiation. Materials Chemistry and Physics 134 (2012) 464-477.
[28] S Khamlich, Z Abdullaeva, JV Kennedy, M Maaza. High performance symmetric supercapacitor based on zinc hydroxychloride nanosheets and 3D graphene-nickel foam composite. Applied Surface Science 405 (2017) 329-336.
[29] SA Abdul Aziz, JV Kennedy, PP Murmu, F Fang, P Cao. Structural and compositional characterization of ion beam sputtered hydroxyapatite thin films on Ti-6Al-4v. Asian Journal of Applied Sciences 7 (2014) 745-752.

[30] PB Johnson, VJ Kennedy, A Markwitz, CR Varoy, N Dytlewski, KT Short. Uptake of light elements of nanoporous layers formed by helium ion implantation. Nucl. Instr. and Meth. in Phys. Res. B 206 (2003) 1056–1061.
[31] E Manikandan, MK Moodley, SS Ray, BK Panigrahi, R Krishnan, N Padhy.. Zinc oxide epitaxial thin film deposited over carbon on various substrate by pulsed laser deposition technique. J Nanoscience & Nanotechnology 10 (2010) 5602-5611.
[32] K. Lokesh, G. Kavitha, E. Manikandan, G Mani, J B B Rayappan, R Ladchumananandasivam, M Maaza. Effective Ammonia Detection Using n-ZnO/p-NiO Heterostructured Nanofibers. IEEE Sensors Journal 16 (2016) 2477 - 2483.
[33] J Kennedy, J Leveneur, A Markwitz. High temperature annealing effects on low energy iron implanted SiO_2. Nucl. Instr. and Meth. in Phys. Res. B 273 (2012) 182-185.